Novel applications of objective measures in cochlear implants

Dong, Y.

Chapter 4

Predicting speech performance in individuals with cochlear implants, based on temporal firing properties of auditory nerve fibers derived from eCAPs

Yu Dong, Jeroen J. Briaire, H. Christiaan

Stronks and Johan H. M. Frijns

Ear and Hearing (under review)

Abstract

Objectives： Many studies have assessed the performance of individuals with cochlear implants (CIs) with electrically evoked compound action potentials (eCAPs). These eCAP-based studies have focused on the amplitude information of the response, without considering the temporal firing properties of excited auditory nerve fibers (ANFs). These temporal features have been associated with neural health in animal studies and, consequently, could be of importance to clinical CI outcomes. With a deconvolution method, combined with a unitary response, the eCAP can be mathematically unraveled into the compound discharge latency distribution (CDLD). The CDLD reflects both the number and the temporal firing properties of excited ANFs. The present study aimed to determine to what extent the temporal properties of eCAPs (quantitatively analyzed in the CDLD) are related to speech perception in individuals with CIs.

Design： This retrospective study acquired data on monosyllabic word recognition scores and intra-operative eCAP amplitude growth functions (AGFs) from 124 adult patients with post-lingual deafness that received the Advanced Bionics HiRes 90K device. The CDLD was determined for each recorded eCAP waveform by deconvolution. Each of the two Gaussian components of the CDLD was described by three parameters: the amplitude, the firing latency (the average latency of each component of the CDLD), and the variance of the CDLD components (an indication of the synchronicity of excited ANFs). The area under the CDLD curve (AUCD) was indicative of the total number of excited ANFs over time. The slope of the AUCD growth function indicated the increases in the number of excited ANFs in response to increasing stimulus levels. Associations between speech perception and each of these CDLD parameters were investigated with linear mixed modeling.

Results: In individuals with CIs, speech perception was significantly associated with the amplitudes of the two CDLD components: the AUCD and the slope of the AUCD growth function, but not with the CDLD latencies. In addition, speech perception was significantly associated with the latency variance in the early CDLD component, but not with the latency

variance in the late CDLD component. Compared to the eCAP amplitude and the slope of the AGF, the amplitude and variance of the first CDLD component, the AUCD and the slope of the AUCD growth function provided a similar explanation of the variance in speech perception but with a higher significance level.

Conclusions： The results demonstrated that both the number and the neural synchrony of excited ANFs, revealed by CDLDs, were indicative of post-implantation speech perception in individuals that received CIs. The CDLD-based parameters could provide a higher significance than the eCAP amplitude or the AGF slope. The authors concluded that CDLDs might serve as a clinical predictor of the survival of ANFs and postoperative speech perception performance. Thus, it would be worthwhile to incorporate the CDLD into eCAP measures in future clinical applications.

Keywords: Cochlear implants; Sensorineural hearing loss; Electrically evoked compound action potential; Temporal firing properties; Speech perception; Neural synchronicity

4.1 Introduction

A cochlear implant (CI) is an implantable device that can partially restore the hearing ability of patients with severe sensorineural hearing loss. Although speech perception capabilities of patients with CIs have improved dramatically over the years, speech outcomes of patients with CIs have been quite unpredictable and variable (van Dijk et al. 1999; Turner et al. 2002; van Eijl et al. 2017). An important factor that affects the speech outcomes of patients with CIs is the condition of the auditory nerve. The neural responses generated by auditory nerve fibers (ANFs) can be evaluated by measuring electrically evoked compound action potentials (eCAPs) in patients with CIs (Fayad & Linthicum 2006; Kim et al. 2010; Garadat et al. 2012; Ramekers et al. 2015; He et al. 2017). The eCAP is typically assessed by examining its amplitude; namely, the difference between the first negative peak (N1) and the first positive peak (P1) (e.g., Lai & Dillier 2000; Kim et al. 2010). This amplitude is thought to be approximately proportional to the

number of ANFs that responded to the stimulus pulse (e.g., McKay et al. 2013; Seyyedi et al. 2014).

Early studies have investigated whether eCAPs could be used to predict speech perception of patients with CIs after implantation. For instance, DeVries et al. (2016) reported that subjects with large eCAP amplitudes tended to show better speech perception scores. Some studies have looked at the slope of the eCAP amplitude growth function (AGF). Steeper AGF slopes, i.e., a faster rate of increase in eCAP amplitude with rising stimulus levels, were associated with a higher density of surviving ANFs (e.g., Kim et al. 2010; He et al. 2017). Moreover, some studies (Brown et al. 1990; Kim et al. 2010) found that steeper AGF slopes were associated with better speech performance, but in other studies, this result was not reproduced (Franck & Norton 2001; Turner et al. 2002; Cosetti et al. 2010). In most studies, the temporal firing properties of excited ANFs that underlie eCAPs were not taken into consideration. However, the eCAP waveforms reflect the temporal firing properties of the excited ANF population (e.g., Goldstein & Kiang 1958; Versnel et al. 1992; Miller et al. 1997). It has been suggested that these temporal firing properties may hold predictive value for anticipating future ANF survival and function (e.g., Miller et al. 1997; Strahl et al. 2016) and potential speech outcomes in individuals with CIs (Pichora-Fuller et al. 2007; Dong et al. 2020).

To extract the temporal firing properties from human eCAPs, an iterative deconvolution method was proposed (Dong et al. 2020, 2021), which assumed that all ANFs had the same unitary response (Fig. 4.1) (Goldstein & Kiang 1958; Versnel et al. 1992). In this method, each eCAP was reconstructed by convolving the unitary response with a parameterized compound discharge latency distribution (CDLD). The CDLD represents the sum of the unitary responses of all individual excited ANFs over time. The simulated eCAP was optimized to match the recorded eCAP by iteratively adjusting the variables in the parameterized CDLD. A two-Gaussian component CDLD was described, as shown in Eq. 4.1 (Fig. 4.1).

$$\mathrm{CDLD_p} = \alpha_1 * \mathrm{N}(\mu_1, \sigma_1) + \alpha_2 * \mathrm{N}(\mu_2, \sigma_2) \tag{4.1}$$

where N represents the Gaussian distribution; the variables α_1, μ_1 and σ_1 belong to the early Gaussian component (in time), and the variables α_2, μ_2 and σ_2 belong to the late Gaussian component. The α_1 and α_2 are the peak amplitudes; the μ_1 and μ_2 are the peak latencies, representing the average firing latencies of excited ANFs; and the σ_1 and σ_2 are the peak widths, which indicate the degree of synchronicity in excited ANFs. The early and late components of CDLDs may be attributed to the excitation of the proximal and peripheral axonal processes of ANFs, respectively (e.g., Stypulkowski & van den Honert 1984; Lai & Dillier 2000; Dong et al. 2020), or due to separate neural responses of part of the ANF population (Ramekers et al. 2015; Konerding et al. 2020). The CDLD can be used to reveal eCAP characteristics, in terms of the number and temporal firing properties of excited ANFs (Fig. 4.1). Specifically, the α_1 and α_2 indicate the neural firing density. These parameters are highly related to the number of excited ANFs and the eCAP amplitude (Strahl et al. 2016; Dong et al. 2020). The number of excited ANFs could be estimated with the area under the CDLD (AUCD) more accurately than with the eCAP amplitude (Dong et al. 2020). Similar to the AGF, the AUCD growth function (AUGF) can be calculated by plotting the AUCD as a function of the stimulus level. The slope of the AUGF indicates the rate of increase in the number of excited ANFs with rising stimulus levels. Previous studies have not considered these temporal firing properties in explorations of whether speech perception was associated with eCAPs after a CI implantation.

In the present study, we aimed to find out to what extent speech perception performance in individuals with CIs can be explained by the temporal firing properties of excited ANFs that are represented in eCAPs. To that end, the CDLD was determined from intraoperatively recorded eCAP waveforms, based on an iterative deconvolution method (Dong et al. 2021). We investigated whether the eight parameters of Eq. 4.1 were correlated with speech perception in individuals after CI implantation. To facilitate comparisons with existing literature, we also compared the predictive value of these eight parameters with the predictive values determined with conventional methods, based on the eCAP amplitude and the AGF slope. The results might provide a new clinical predictor of ANF survival and postoperative speech perception

performance.

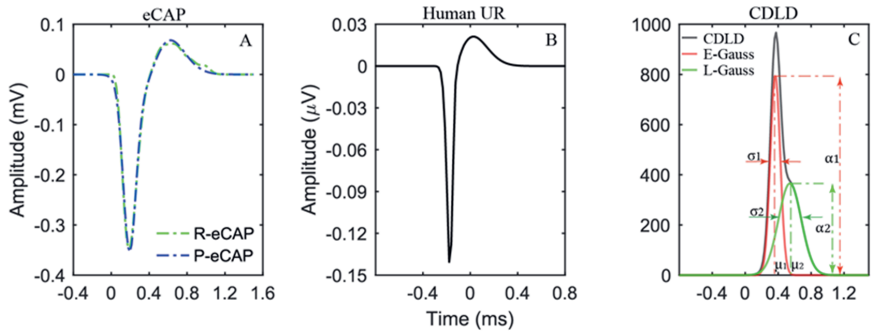

Fig. 4.1 Extraction of the temporal firing properties of excited auditory nerve fibers from eCAPs, based on an iterative deconvolution method proposed by Dong et al. (2020, 2021). In this method, an eCAP (A, blue line) was calculated by convoluting a human unitary response (UR) (B) and a parameterized CDLD (C), optimized to match a recorded eCAP (A, green line), and iteratively minimizing the fitting error. This CDLD (C) consists of early and late Gaussian components; the parameters of the early component (α1, μ1, and σ1) and the late component (α2, μ2, and σ2) reflect the temporal firing properties. eCAP: electrically evoked compound action potential; R-eCAP: recorded eCAP; P-eCAP: predicted eCAP; CDLD: compound discharge latency distribution; E-Gauss: early Gaussian component; L-Gauss: late Gaussian component.

4.2 MATERIAL AND METHODS

4.2.1 Patient Population

This retrospective study included AGF recordings from 134 adult patients with post-lingual deafness that had undergone CI implantation at the Leiden University Medical Center between June 2012 and March 2019. The AGF was recorded as part of the standard clinical routine for assessing CI function intraoperatively. All patients received unilateral implants with a HiRes90K device, with either a HiFocus-1J or a HiFocus Mid-Scala electrode array (Advanced Bionics, Valencia, CA). These electrode arrays consisted of 16 electrode contacts (numbered from 1 to 16, in apical to basal order). According to the inclusion criteria of eCAPs, 10 patients were

excluded (see Data Recordings). Therefore, the remaining 124 patients were included in the analysis. Table 4.1 shows the characteristics of the included patients.

TABLE 4.1. Characteristics of patients with cochlear implants due to post-lingual deafness

Characteristic	Patients (n = 124)
Sex	
Male	49
Female	75
Cochlear implant type	
HiRes90K 1J	19
HiRes90K Mid-Scala	105
Mean age at implantation, years	61.3 ± 19.2
Mean duration of deafness, years	14.1±13.7
Etiology	
Ototoxic Medication	3
Meniere's disease	2
Meningitis	8
Otosclerosis	7
Usher syndrome	2
Congenital/Hereditary (non-specified)	37
Other/Unknown	65
Monosyllabic word scores at 1 year, % correct	60.8 ± 21.1

Values are the number of patients or mean ± SD, as indicated.

4.2.2 Data Recordings

4.2.2.1 Test Procedure for AGFs

The AGFs were recorded on all odd electrode contacts with the forward-masking paradigm

provided in the Research Studies Platform Objective Measures software program (Advanced Bionics, Sylmar, CA). The electrical stimulus for the masker and probe was a monopolar, cathodic-first, charge-balanced, biphasic pulse (32 μs/phase). The interval between the masker and probe pulses was fixed at 400 μs. The eCAP response was recorded at a sampling rate of 56 kHz and a gain of 300. For each eCAP, 32 averages were performed. Each AGF was based on ten different current levels, ranging from 50 to 500 clinical units (CU). Additional details on the recordings were described previously (Biesheuvel et al. 2017; Dong et al. 2020).

The N1 and P1 peaks of eCAP waveforms were defined as the minimum and maximum amplitudes, respectively, measured across the 180 to 490 μs and the 470 to 980 μs intervals after the end of stimulation. The eCAP amplitude was defined as the voltage difference between P1 and N1 (mV). The noise level of the recording was determined from the last 30 samples of the recording, with the assumption that no remaining neural response or stimulus artifact was present in this section (for details, see Dong et al. 2021). The signal-to-noise ratio of the eCAP was calculated as the eCAP amplitude divided by the root mean square of the noise segment. Valid eCAPs were selected using a semiautomatic method programmed in MATLAB (Mathworks 2019a, Natick, MA, USA), which included two criteria: the eCAP amplitude had to be larger than 25 μV, and the signal-to-noise ratio had to exceed +15 dB. eCAPs that did not meet both of these criteria were excluded. As a result, we included 5612 eCAPs obtained from 920 AGFs originating from 124 patients (3588 recordings were excluded) for further analysis.

We performed linear regression on the AGF data to extract the slope of the best-fit regression line (μV/CU). The intercept of the line with the x-axis is defined as the eCAP threshold (for details see Biesheuvel et al. 2017). An example of an AGF and its underlying recordings is shown in Fig. 4.2.

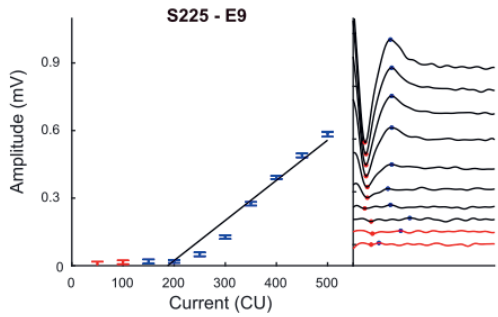

Fig. 4.2 Example of an AGF from the subject S225, obtained at electrode 9. The AGF (left) shows the eCAP amplitude as a function of stimulus intensity. The corresponding eCAPs (right) are plotted from low (bottom) to high (top) stimulus intensity. Data points that did not show true eCAP responses are shown in red, and points included in the AGF are shown in blue. Error bars reflect the variance in eCAP amplitude. AGF: amplitude growth function; eCAP: electrically evoked compound action potential.

4.2.2.2 Extraction of the Temporal Firing Properties in eCAPs

To deduce the temporal firing properties of excited ANFs from eCAPs, we calculated CDLDs from eCAP waveforms with an iterative deconvolution method (for details see Dong et al. 2020, 2021). Before we calculated CDLDs, the eCAP waveforms of AGFs were pre-processed. First, the baseline was corrected to zero, with the noise level as a reference. Second, to circumvent mathematical problems, due to the convolutions, 50 additional samples were added to the start and end of the recorded waveforms by performing a linear extrapolation to zero. Then, the pre-processed eCAPs were entered as input into the iterative deconvolution procedure to obtain CDLDs. Specifically, we simulated the eCAPs as the convolution of the human unitary response calculated by Dong et al. (2020) with a parameterized CDLD (Eq. 4.1), with a deconvolution fitting error minimization routine (Fig. 4.1). In this routine, the human unitary response was constant and the simulated eCAP was optimized by iteratively adjusting the variables in the parameterized CDLD, until the simulated eCAP converged to the recorded eCAP. We validated the goodness of fit by calculating the normalized root mean square error. Then, the temporal firing properties were revealed, based on the CDLD parameter values, as shown in Equation 4.1.

To estimate the number of excited ANFs, the AUCD was calculated by taking the integral of CDLDs over time. We applied linear regression techniques to the AUCD data and extracted the slope of the AUGF (number of fibers/CU) from the best-fit regression line. All signal processing was performed offline, with MATLAB (Mathworks 2019a, Natick, MA, USA).

4.2.3 Evaluation of Speech Perception

Speech perception was evaluated at predetermined intervals during a standard clinical follow-up. In this study, we analyzed the word recognition score, obtained in a quiet environment, at 1 year after implantation. Speech material comprised the standard Dutch speech test of the Dutch Society of Audiology. It consisted of phonetically balanced monosyllabic (CVC) word lists (Bosman & Smoorenburg, 1995), presented at 65 dB SPL in a quiet listening environment. To enhance test reliability, four lists (44 words) per condition were performed. All speech testing was conducted in a soundproof room, with a calibrated sound-speaker, with the patient in a frontal position at a meter distance. All patients used the HiRes processing strategy from Advanced Bionics.

4.2.4 Statistical Analysis

LMMs were constructed with the lme4 package in R (R version 3.6.1, The R Foundation for Statistical Computing, 2020). Word recognition outcomes were assumed to be the sum of fixed and random effects. Because random effects often introduce correlations between cases, they should be taken into account to elucidate the fixed effects, which affect the population. The LMM allowed the inclusion of potential confounding factors (Brauer & Curtin 2017; Bolker et al. 2009). Moreover, the LMM design accounted for missing data (Fitzmaurice et al. 2004; Netten et al. 2017).

LMMs were used to test the relationship between the word recognition score and the metrics based on CDLDs obtained from Eq. 4.1, the AUCD, and the slope of AUGF. Our dataset included only a single word recognition score per patient, but multiple eCAP measurements were obtained

in each patient (see Data Recordings). Therefore, each of the eight CDLD-related metrics was entered as the dependent variable in a separate LMM. In each of these models, the word recognition score was entered as a fixed covariate. Five additional fixed factors were included that could potentially affect the word recognition score and the CDLD-related parameters, including (1) the implant design, (2) the contact location along the electrode array, (3) the current level, (4) the age at implantation, and (5) the duration of deafness. The duration of deafness was defined as the time, in years, between the age at implantation and the age at which patients had experienced severe hearing loss, either in both ears or in the second ear. Data on the duration of deafness were available for 93 patients. The subject IDs were entered as random categorical variables, including a random intercept (Brauer & Curtin 2017). A p-value < 0.05 was considered to reflect a statistically significant difference.

To compare the CDLD-related parameters to the eCAP amplitude and the AGF slope in their abilities to explain the variance in word recognition scores, the corresponding R^2 was required. However, the LMMs did not produce an R^2 estimate. Thus, we performed simple linear regression, and we calculated the R^2 as the square of the coefficient of correlation (Neter et al. 1996; Khan et al. 2005). In these analyses, the parameters were averaged across all odd electrodes and/or suprathreshold current levels within each patient, as described in previous studies (e.g., Franck & Norton 2001; He et al. 2017).

To provide visual representations, word recognition scores were plotted against the corresponding CDLD-related parameters, the eCAP amplitude, and the AGF slope, which were averaged across electrodes and/or current levels within each patient. Of note, these plots did not completely match the analyses performed with LMMs, because the models took into account missing data points and random effects.

4.3 RESULTS

4.3.1 Derivation of CDLDs

We derived the CDLD from each eCAP waveform. Figure 4.3 shows three examples of eCAP waveforms and their corresponding CDLDs, each with two Gaussian components. Overall, the 95% confidence intervals of the goodness of fit (i.e., the normalized root mean square error) ranged from 0.91 to 0.96. Table 4.2 shows the mean values (with standard deviations) of the CDLD parameters.

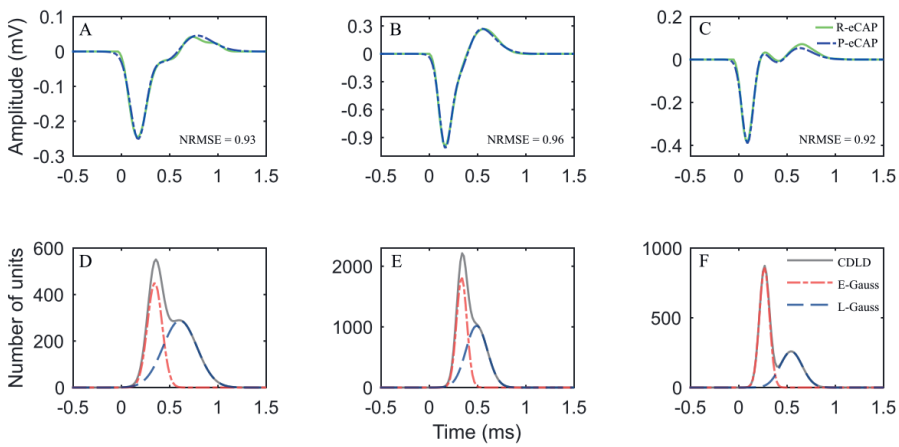

Fig. 4.3 Examples of eCAPs with different morphologies (upper row) and corresponding CDLDs (lower row). eCAP: electrically evoked compound action potential; R-eCAP: recorded eCAP; P-eCAP: predicted eCAP; CDLD: compound discharge latency distribution; E-Gauss: early Gaussian component; L-Gauss: late Gaussian component. NRMSE: normalized root mean square error.

4.3.2 Relationship between CDLDs and Speech Perception

At one year of follow-up, the average monosyllabic word score for the 124 adult patients with CIs was 60.8% ± 21.1% correct. Table 4.3 shows the parameter estimates for the eight LMMs, with the word recognition score as the independent variable and the CDLD parameters as dependent variables.

The LMM analysis revealed significant positive associations between α_1 and α_2 and the word recognition score ($F(1, 117.1) = 8.7$, $p = 0.003$; $F(1, 117) = 5.6$, $p = 0.01$, respectively). These outcomes suggested that patients with a higher word recognition score tended to have larger α_1 and α_2 values. Among the remaining factors, the implant design, current, and contact location showed a significant effect on α_1 and α_2 ($p < 0.05$), but the duration of deafness and age at implantation did not affect α_1 ($p = 0.07$; $p = 0.25$) or α_2 ($p = 0.17$; $p = 0.51$).

TABLE 4.2. CDLD parameters for eCAPs in patients with cochlear implants

Parameters	α_1	α_2	μ_1 (ms)	μ_2 (ms)	σ_1 (ms)	σ_2 (ms)	AUCD (number of fibers)	AUGF slope (number of fibers/CU)
Mean	710	553	0.37	0.59	0.076	0.16	484	0.52
SD	46	69	0.049	0.1	0.03	0.066	142	0.07

Means represent averaged values over all electrodes and/or over all stimulation levels and for all patients; CDLD: compound discharge latency distribution; eCAPs: evoked compound action potentials; AUCD: area under the CDLD curve; AUGF: the AUCD growth function.

The AUCD, an estimate of the number of excited ANFs in each recorded eCAP, was significantly correlated with the word recognition score ($F(1,122.1) = 8.1$, $p = 0.005$). This result indicated that when more ANFs were excited, better speech perception was achieved. The implant design, current level, and contact location showed significant effects on the AUCD (all $p < 0.01$), but the duration of deafness and age at implantation did not affect the AUCD (all $p > 0.2$).

The slope of the AUGF was significantly correlated with the word recognition score ($F(1,122.1) = 8.7$, $p = 0.004$). The AUGF slope was significantly affected by the electrode location ($p < 0.001$), but not by the other factors (all $p > 0.05$).

We found that the μ_1 and μ_2, reflecting the average firing latencies of excited ANFs, were not significantly associated with the word recognition score ($F(1, 116) = 0.87$, $p = 0.82$; $F(1, 113.6) = 1.6$, $p = 0.2$, respectively). The contact location showed a significant effect on μ_1 and μ_2 (both $p < 0.001$). The age at implantation had a positive effect on μ_2 ($p = 0.02$), but not on μ_1

($p = 0.53$). The duration of deafness and the current level did not significantly affect μ_1 ($p = 0.17$ and $p = 0.06$, respectively) or μ_2 ($p = 0.3$ and $p = 0.09$, respectively).

The σ_1 and σ_2 represented the degree of neural synchronicity. The LMMs showed that σ_1 was significantly negatively associated with the word recognition score ($F(1, 107.7) = 6.5$, $p = 0.01$). However, σ_2 was not significantly associated with the word recognition score ($F(1,113) = 3.5$, $p = 0.06$). The implant design, current level, electrode location, and deafness duration showed significant effects on σ_1 and σ_2 (all $p < 0.05$). The age at implant showed a significant effect on σ_2 ($p < 0.001$), but not on σ_1 ($p = 0.1$).

TABLE 4.3. Parameter estimates from LMMs, with the word recognition score as the independent variable, and the CDLD parameters as dependent variables

Dependent variable	Estimate	SD	F	p-value
α_1	+18	5.6	8.7	0.003*
α_2	+13	5.4	5.6	0.01*
μ_1	-0.011	0.057	0.07	0.82
μ_2	-0.07	0.06	1.02	0.2
σ_1	-0.09	0.039	6.5	0.01*
σ_2	-0.1	0.052	3.5	0.06
AUCD	+15	5.1	8.1	0.005*
AUGF slope	+0.18	0.06	8.7	0.004*

*LMM: linear mixed model; CDLD: compound discharge latency distribution; AUCD: area under the CDLD curve; AUGF: the AUCD growth function; SD: standard deviation; *Significant difference.*

4.3.3 Abilities of CDLD Parameters, eCAP Amplitude, and AGF Slope to Explain the Variance in Speech Perception

We performed simple linear regression analyses to determine whether the CDLD-related

parameters explain R^2, the variability in the word recognition score better than the eCAP amplitude, and the slope of AGF (Table 4.4). For these analyses, the CDLD parameters were calculated for each individual patient as the average of all available eCAPs, across different electrode contacts and current levels. α_1 and α_2 showed R^2 values of 0.102 and 0.05, respectively (Fig. 4.4). The AUCD showed an R^2 value of 0.12 (Fig. 4.5A). The AUGF slope showed an R^2 value of 0.09 (Fig. 4.5B). μ_1 and μ_2 revealed small R^2 values, 0.0009 and 0.015, respectively. σ_1 showed a moderately high R^2 of 0.09 (Fig. 4.6A), but σ_2 showed a low value of 0.04 (Fig. 4.6B).

The eCAP amplitude, calculated for each individual patient as the average of all available eCAPs across different electrode contacts and current levels, showed an R^2 of 0.06 (Fig. 4.7A). The AGF slope showed an R^2 of 0.07 (Fig. 4.7B). It was calculated for each patient as the average of all available AGFs across different contacts.

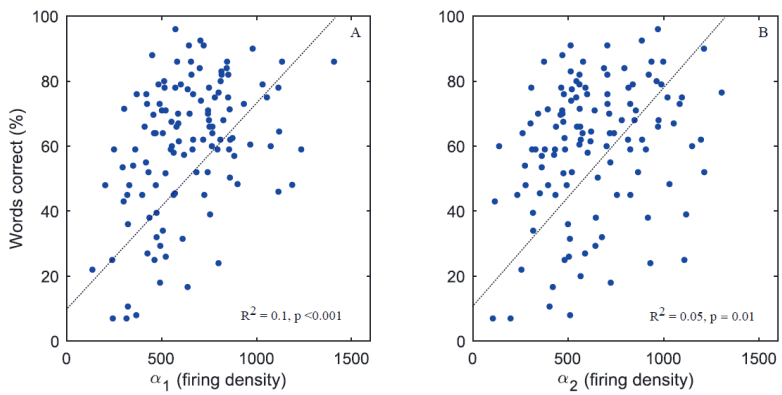

Fig. 4.4 Correlations between word recognition scores and firing density parameters. The percentage of words recognized by each individual patient are plotted against the corresponding α_1 (A) and α_2 (B) values, averaged across all contacts and all current levels. R^2 values are derived from the linear regressions (dotted lines).

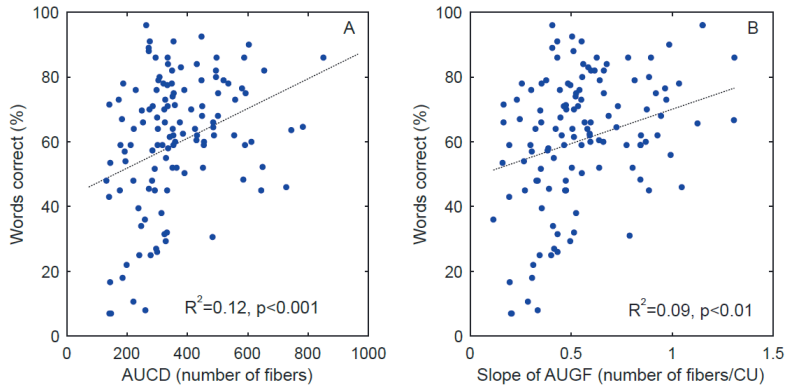

Fig. 4.5 Correlations between word recognition scores and the number of ANFs and AUGF slope. The percentage of words recognized by each individual patient are plotted against the corresponding AUCD (A) and AUGF slope (B), averaged across all contacts and/or all current levels. R^2 values are derived from the linear regressions (dotted lines). ANF: auditory nerve fiber; AUCD: area under the CDLD curve; CDLD: compound discharge latency distribution; AUGF: the AUCD growth function.

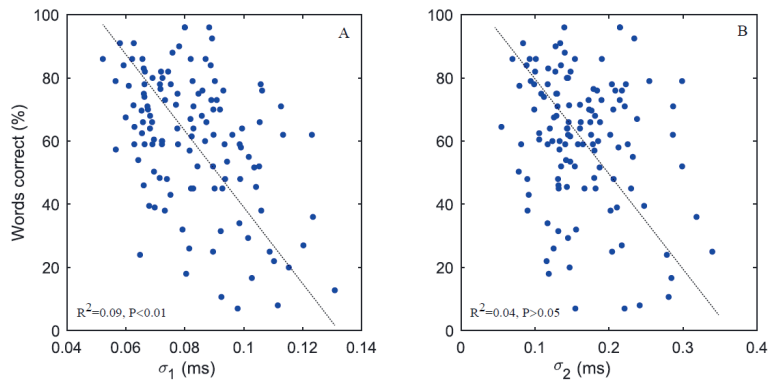

Fig. 4.6 Correlations between word recognition scores and neural synchronicity parameters. The percentage of words recognized by each individual patient are plotted against the corresponding σ_1 (A) and σ_2 (B) values, averaged across all contacts and all current levels. R^2 value is derived from the linear regression (dotted line).

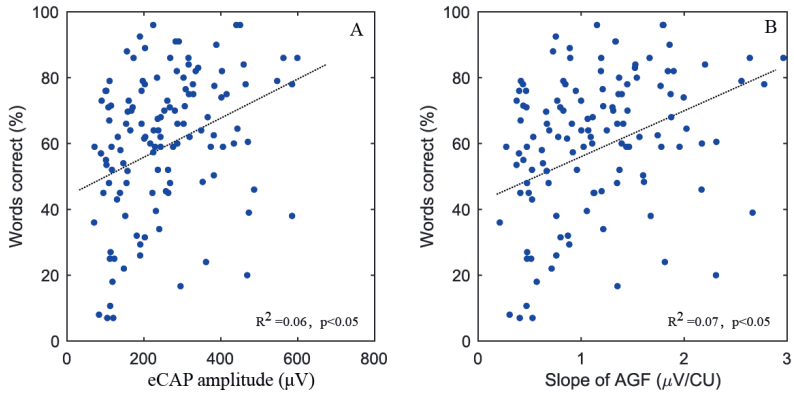

Fig. 4.7 Correlations between word recognition scores and eCAP parameters. The percentage of words recognized by each individual patient are plotted against the corresponding eCAP amplitude (A) and AGF slope (B), averaged across all electrodes and/or current levels. R^2 values are derived from the linear regressions (dotted lines). eCAP: electrically evoked compound action potential; AGF: amplitude growth function.

TABLE 4.4. Comparison of the abilities of different parameters to explain (R^2) the variance in speech performance in patients with cochlear implants

Parameters	R^2
α_1	0.1
α_2	0.05
μ_1	0.0009
μ_2	0.015
σ_1	0.09
σ_2	0.04
AUCD	0.12
AUGF slope	0.09
eCAP amplitude	0.06
AGF slope	0.07

AUCD: the area under the CDLD curve; CDLD: compound discharge latency distribution; AUGF: the AUCD growth function; eCAP: electrically evoked compound action potential; AGF: the eCAP amplitude growth function. R2 values are derived from the linear regressions.

4.4 DISCUSSION

This study was the first to test whether the CDLD (i.e., the number and the temporal firing

properties of excited ANFs in human eCAPs) was correlated with speech understanding. We showed that speech perception performance was significantly associated with the CDLD parameters related to the number of excited ANFs (α_1, α_2, AUCD), with the AUGF slope (i.e., the speed of the increase of the number of excited ANFs with increasing stimulus), and with early neural synchronicity (σ_1). The other three parameters (μ_1, μ_2 and σ_2) were not significantly correlated with speech recognition. Moreover, we found that the CDLD-based AUCD, AUGF slope, and the α_1 and σ_1 parameters provided a higher significance level than the two classically applied measures of eCAP (the amplitude and the AGF slope), in terms of predicting speech perception.

Results from post-mortem studies have suggested that patients with a greater number of surviving ANFs tended to perform better in speech recognition tests (e.g., Otte et al. 1978; Kawano et al. 1998; Khan et al. 2005; Seyyedi et al. 2014). After studies showed that eCAPs could be indicative of neural survival, interest increased in using eCAP measurements to evaluate correlations with speech perception (e.g., Shepherd & Javel 1997; He et al. 2017). However, needless to say, a direct comparison between the eCAP amplitude and the number of surviving ANFs in individuals with CIs was impossible. In this study, the temporal firing properties of excited ANFs extracted from the CDLD metrics in eCAPs (α_1, α_2, AUCD) provided a more accurate estimate of the number of functional ANFs than the eCAP amplitude (Dong et al. 2020), and the AUGF slope provided a more accurate rate of the increase of the number of excited ANFs with increasing stimulus than AGF slope. The significant associations between the word recognition score and these four metrics (Table 4.3) supported the notion that more functional fibers would provide better speech perception. According to the results in the present study, combined with those in previous animal studies, we conclude that the number of surviving ANFs played a significant role in speech perception performance. In other words, a larger number of healthy spiral ganglion cells could potentially lead to higher speech perception scores after cochlea implantation in a given patient.

Earlier studies have suggested that a decline in the synchronicity of the auditory neural response

might adversely influence speech understanding (e.g., Hellstrom & Schmiedt 1990; Pichora-Fuller et al. 2007). This theoretical expectation was substantiated for the first time in our study. Specifically, we showed that the σ_1 was negatively associated with speech perception (Table 4.3), that is, a more synchronous ANF response in the early CDLD peak (lower σ_1) was associated with better speech understanding. Moreover, although the σ_2 was not significantly associated with speech perception (p=0.06), a similar trend was observed (Fig. 4.6B). Our findings were consistent with previous findings that showed that a decline in the synchronicity of excited ANFs was associated with different factors (e.g., the duration of deafness, auditory nerve abnormalities, and myelin disorders) (Shepherd & Javel 1997; Rance 2005), and in turn, these factors may lead to a deterioration in CI speech outcomes. Our analysis of σ suggested that different eCAP waveforms with the same amplitudes, but different shapes could have clinical implications about neural synchrony and speech performance. That is, patients with narrower eCAP waveforms tended to have greater neural synchrony and better speech performance than those with wider eCAP waveforms.

To our knowledge, no previous study has reported that the peak latency of eCAPs was associated with speech perception performance in patients with CIs. Also in our study, we did not observe significant associations between the average firing latencies of excited ANFs in CDLDs (μ_1 and μ_2) and speech perception outcomes indicating that firing latencies of excited ANFs had little effect on speech perception (Table 4.3).

Previous studies have reported that patients with larger eCAP amplitudes and steeper AGF slopes tended to show better speech perception than their counterparts (e.g., Brown et al. 1990; Kim et al. 2010; DeVries et al. 2016). In line with their findings, we found that eCAP amplitudes and steeper AGF slopes were significantly associated with speech perception (Fig. 4.7). Compared with the eCAP amplitude and AGF slope we found that a similar proportion of the variance in speech perception could be explained by the α_1, AUCD, AUGF slope and σ_1 (Table 4.4), but because of the higher significance levels (Table 4.3 and Fig. 4.7), α_1, AUCD, AUGF slope and σ_1 might be better predictors of CI outcomes than the traditionally used eCAP amplitude and

AGF slope.

Of note, the CDLD parameters showed relatively low abilities to explain the variance in speech perception. Although this finding did not diminish the importance of the number and neural synchrony of excited ANFs, nevertheless, it suggested that a good number of nerves and good neural synchronicity alone would not be sufficient to guarantee a good CI outcome, because other factors must also play a role in speech recognition, including but not limited to the duration of deafness and cognitive ability (e.g., Fayad et al. 2006; He et al. 2017; Pisoni et al. 2017). In our data, we also observed that patients who have undergone a longer period of deafness showed significantly poorer speech perception performance than their counterparts. In these cases, the number of surviving peripheral fibers would be less relevant with speech recognition.

A reliable derivation of the temporal firing properties of ANFs in eCAPs was highly related to the shape of the human unitary response, as stated in Dong et al. (2020). The human unitary response has not been recorded in humans, and the one used in this study was estimated with iterative deconvolution by Dong et al. (2020, 2021) (Fig. 4.1B). In addition, the CDLD provides a valid estimate of the number of excited ANFs, only when the two components of CDLDs originate from two different groups of ANFs. However, this issue remains controversial, because the two CDLD components may, to some extent, originate from the same group of spiral ganglion cells (Ramekers et al. 2015; Konerding et al. 2020). For instance, the origin of the early component of CDLDs may be attributable to the direct excitation of the axonal process in the modiolus proximal to the spiral ganglion cell; and the origin of the late component of CDLDs may be attributable to the activation of the axonal process peripheral to the soma of the bipolar ganglion neuron (e.g., Stypulkowski & van den Honert 1984; Lai & Dillier 2000). Further anatomical and electrophysiological studies are warranted to obtain insight into the physiological mechanism underlying the unitary response and the CDLD. This knowledge could provide a deeper understanding of how the two CDLD components affect speech performance in individuals with CIs.

To date, eCAP measurements have proven to be useful in diagnosing and managing CI failures, although some discrepancies have been reported (Gantz et al. 1988; Hughes et al. 2004; van Eijl et al. 2017; DeVries et al. 2016; He et al. 2017). Our results demonstrated that the extraction of CDLDs from eCAP waveforms can provide additional clinical information, including the number and synchronicity of excited ANFs and how they affect speech understanding after cochlear implantation. Therefore, integrating the extraction of CDLDs into eCAP measurements may provide a potential predictor of CI outcomes.

4.5 CONCLUSIONS

The results of this study showed that, in individuals with CIs, speech perception after implantation was significantly associated with the number and synchronicity of excited ANFs, measured in eCAPs. We found that the CDLD-related parameters could explain a similar variance in speech perception but with a higher significance than the eCAP amplitude and the AGF slope. We conclude that eCAP-derived CDLD measurements, which reflect the temporal features of excited ANFs, could potentially serve as additional predictors of speech perception performance in individuals with CIs.

ACKNOWLEDGMENTS

The first author of the present study was financially supported by the China Scholarship Council. There are no conflicts of interest, financial, or otherwise.

Yu Dong designed and conducted experiments, analyzed data, and wrote the manuscript; Jeroen J. Briaire designed experiments, discussed the results and implications, and provided critical revision. H. Christiaan Stronks discussed the results and implications and provided critical revision; Johan H. M. Frijns discussed the results and implications and provided critical revision.

We are grateful to Nicolaas. R. A. van Groesen and Stefan Boehringer at the Leiden University Medical Center for statistical consultations on the data analysis. We would also like to thank Jan Dirk Biesheuvel for his assistance with preprocessing the raw eCAP data.

REFERENCES

Abbas, P. J., & Brown, C. J. (1991). Electrically evoked auditory brainstem response: refractory properties and strength-duration functions. *Hearing research*, *51*(1), 139-147.

Biesheuvel, J. D., Briaire, J. J., & Frijns, J. H. (2018). The precision of eCAP thresholds derived from amplitude growth functions. *Ear and hearing*, *39*(4), 701-711.

Bolker, B. M., Brooks, M. E., Clark, C. J., Geange, S. W., Poulsen, J. R., Stevens, M. H. H., & White, J. S. S. (2009). Generalized linear mixed models: a practical guide for ecology and evolution. *Trends in ecology & evolution*, *24*(3), 127-135.

Bosman, A. J., & Smoorenburg, G. F. (1995). Intelligibility of Dutch CVC syllables and sentences for listeners with normal hearing and with three types of hearing impairment. *Audiology*, *34*(5), 260-284.

Brauer, M., & Curtin, J. J. (2018). Linear mixed-effects models and the analysis of nonindependent data: A unified framework to analyze categorical and continuous independent variables that vary within-subjects and/or within-items. *Psychological Methods*, *23*(3), 389.

Brown, C. J., Abbas, P. J., & Gantz, B. (1990). Electrically evoked whole‐nerve action potentials: Data from human cochlear implant users. *The Journal of the Acoustical Society of America*, *88*(3), 1385-1391.

Cosetti, M. K., Shapiro, W. H., Green, J. E., Roman, B. R., Lalwani, A. K., Gunn, S. H., ... & Waltzman, S. B. (2010). Intraoperative neural response telemetry as a predictor of performance. *Otology & Neurotology*, *31*(7), 1095-1099.

DeVries, L., Scheperle, R., & Bierer, J. A. (2016). Assessing the electrode-neuron interface with the electrically evoked compound action potential, electrode position, and behavioral thresholds. *Journal of the Association for Research in Otolaryngology*, *17*(3), 237-252.

Dong, Y., Briaire, J. J., Biesheuvel, J. D., Stronks, H. C., & Frijns, J. H. M. (2020). Unravelling the Temporal Properties of Human eCAPs through an Iterative Deconvolution Model. *Hearing Research*, *395*, 108037.

Dong, Y., Stronks, H. C., Briaire, J. J., & Frijns, J. H. M. (2021). An iterative deconvolution model to extract the temporal firing properties of the auditory nerve fibers in human eCAPs. MethodsX, 8, 101240.

Fayad, J. N., & Linthicum, F. H. (2006). Multichannel cochlear implants: Relation of histopathology to performance. *Laryngoscope*, *116*(8), 1310–1320.

Fitzmaurice, G. M., Laird, N. M., & Ware, J. 2. (2004). Linear mixed effects models. *Applied longitudinal*

analysis, *1*, 187-236.

Franck, K. H., & Norton, S. J. (2001). Estimation of psychophysical levels using the electrically evoked compound action potential measured with the neural response telemetry capabilities of Cochlear Corporation's CI24M device. *Ear and Hearing*, *22*(4), 289-299.

Gantz, B. J., Tyler, R. S., McCabe, B. F., Tye-Murray, N., Lansing, C., Kuk, F., Knutson, J. F., Hinrichs, J., Woodworth, G., Abbas, P., & Brown, C. (1988). Evaluation of five different cochlear implant designs: Audiologic assessment and predictors of performance. In *Laryngoscope* (Vol. 98, Issue 10, pp. 1100–1106).

Garadat, S. N., Zwolan, T. A., & Pfingst, B. E. (2012). Across-site patterns of modulation detection: Relation to speech recognition. *The Journal of the Acoustical Society of America*, *131*(5), 4030–4041.

Goldstein, M. H., & Kiang, N. Y. S. (1958). Synchrony of Neural Activity in Electric Responses Evoked by Transient Acoustic Stimuli. *Jasa*, *30*(2), 107–114.

Hall, R. D. (1990). Estimation of surviving spiral ganglion cells in the deaf rat using the electrically evoked auditory brainstem response. *Hearing research*, *49*(1-3), 155-168.

He, S., Teagle, H. F. B., & Buchman, C. A. (2017). The electrically evoked compound action potential: From laboratory to clinic. *Frontiers in Neuroscience*, *11*(JUN), 1–20.

Hellstrom, L. I., & Schmiedt, R. A. (1990). Compound action potential input/output functions in young and quiet-aged gerbils. *Hearing research*, *50*(1-2), 163-174.

Hughes, M. L., Brown, C. J., & Abbas, P. J. (2004). Sensitivity and specificity of averaged electrode voltage measures in cochlear implant recipients. *Ear and hearing*, *25*(5), 431-446.

Khan, A. M., Handzel, O., Burgess, B. J., Damian, D., Eddington, D. K., & Nadol Jr, J. B. (2005). Is word recognition correlated with the number of surviving spiral ganglion cells and electrode insertion depth in human subjects with cochlear implants? *The Laryngoscope*, *115*(4), 672-677.

Kawano, A., Seldon, H. L., Clark, G. M., Ramsden, R. T., & Raine, C. H. (1998). Intracochlear factors contributing to psychophysical percepts following cochlear implantation. *Acta Oto-Laryngologica*, *118*(3), 313–326.

Kim, J. R., Abbas, P. J., Brown, C. J., Etler, C. P., O'Brien, S., & Kim, L. S. (2010). The relationship between electrically evoked compound action potential and speech perception: a study in cochlear implant users with short electrode array. *Otology & neurotology: official publication of the American Otological Society, American Neurotology Society [and] European Academy of Otology and Neurotology*, *31*(7), 1041.

Konerding, W., Arenberg, J. G., Kral, A., & Baumhoff, P. (2020). Late electrically-evoked compound

action potentials as markers for acute micro-lesions of spiral ganglion neurons. *Hearing Research*, 108057.

McKay, C. M., Chandan, K., Akhoun, I., Siciliano, C., & Kluk, K. (2013). Can ECAP measures be used for totally objective programming of cochlear implants?. *Journal of the Association for Research in Otolaryngology*, *14*(6), 879-890.

Miller, C. A., Abbas, P. J., & Robinson, B. K. (1994). The use of long-duration current pulses to assess nerve survival. *Hearing research*, *78*(1), 11-26.

Miller, C. A., Abbas, P. J., Rubinstein, J. T., Robinson, B. K., & Matsuoka, A. J. (1999). The neurophysiological effects of simulated auditory prosthesis stimulation.

Nadol Jr, J. B., Burgess, B. J., Gantz, B. J., Coker, N. J., Ketten, D. R., Kos, I., ... & Shallop, J. K. (2001). Histopathology of cochlear implants in humans. *Annals of Otology, Rhinology & Laryngology*, *110*(9), 883-891.

Neter, J., Kutner, M. H., Nachtsheim, C. J., & Wasserman, W. (1996). Applied linear statistical models.

Netten, A. P., Dekker, F. W., Rieffe, C., Soede, W., Briaire, J. J., & Frijns, J. H. (2017). Missing data in the field of otorhinolaryngology and head & neck surgery: need for improvement. *Ear and hearing*, *38*(1), 1-6.

Otte, J., Schuknecht, H. F., & Kerr, A. G. (1978). Ganglion cell populations in normal and pathological human cochleae. Implications for cochlear implantation. *The Laryngoscope*, *88*(8), 1231-1246.

Pfingst, B. E., Sutton, D., Miller, J. M., & Bohne, B. A. (1981). Relation of psychophysical data to histopathology in monkeys with cochlear implants. *Acta oto-laryngologica*, *92*(1-6), 1-13.

Pisoni, D. B., Kronenberger, W. G., Harris, M. S., & Moberly, A. C. (2017). Three challenges for future research on cochlear implants. *World journal of otorhinolaryngology-head and neck surgery*, *3*(4), 240-254.

Ramekers, D., Versnel, H., Strahl, S. B., Klis, S. F. L., & Grolman, W. (2015). Recovery characteristics of the electrically stimulated auditory nerve in deafened guinea pigs: Relation to neuronal status. *Hearing Research*, *321*, 12–24.

Rance, G. (2005). Auditory neuropathy/dys-synchrony and its perceptual consequences. *Trends in amplification*, *9*(1), 1-43.

Pichora-Fuller, M. K., Schneider, B. A., MacDonald, E., Pass, H. E., & Brown, S. (2007). Temporal jitter disrupts speech intelligibility: A simulation of auditory aging. *Hearing research*, *223*(1-2), 114-121.

Seyyedi, M., Viana, L. M., & Nadol Jr, J. B. (2014). Within-subject comparison of word recognition and spiral ganglion cell count in bilateral cochlear implant recipients. *Otology & neurotology: official*

publication of the American Otological Society, American Neurotology Society [and] European Academy of Otology and Neurotology, *35*(8), 1446.

Shepherd, R. K., & Javel, E. (1997). Electrical stimulation of the auditory nerve. I. Correlation of physiological responses with cochlear status. *Hearing Research*, 108(1–2), 112–144.

Strahl, S. B., Ramekers, D., Marjolijn M. B. Nagelkerke, K. E. S., Spitzer, P., Klis, S. F. L., Grolman, W., & Versnel, H. (2016). Assessing the Firing Properties of the Electrically Stimulated Auditory Nerve Using a Convolution Model. Adv Exp Med Biol, 894.

Stypulkowski, P. H., & van den Honert, C. (1984). Physiological properties of the electrically stimulated auditory nerve. I. Compound action potential recordings. Hearing Research, 14(3), 205–223. https://doi.org/10.1016/0378-5955(84)90051-0

Turner, C., Mehr, M., Hughes, M., Brown, C., & Abbas, P. (2002). Within-subject predictors of speech recognition in cochlear implants: A null result. *Acoustics Research Letters Online*, *3*(3), 95-100.

van de Heyning, P., Arauz, S. L., Atlas, M., Baumgartner, W. D., Caversaccio, M., Chester-Browne, R., ... & Skarzynski, H. (2016). Electrically evoked compound action potentials are different depending on the site of cochlear stimulation. *Cochlear implants international*, *17*(6), 251-262.

van den Honert, C., & Stypulkowski, P. H. (1984). Physiological properties of the electrically stimulated auditory nerve. II. Single fiber recordings. *Hearing Research*, *14*(3), 225–243.

van der Beek, F. B., Briaire, J. J., & Frijns, J. H. (2012). Effects of parameter manipulations on spread of excitation measured with electrically-evoked compound action potentials. *International journal of audiology*, *51*(6), 465-474.

van Dijk, J. E. van Olphen, A. F. Langereis, M. C. Mens, L. H. M. Brokx, J. P. L. & Smoorenburg, G. F. (1999). Predictors of cochlear implant performance. International Journal of Audiology, 38(2), 109–116.

van Eijl, R. H., Buitenhuis, P. J., Stegeman, I., Klis, S. F., & Grolman, W. (2017). Systematic review of compound action potentials as predictors for cochlear implant performance. *The Laryngoscope*, *127*(2), 476-487.

Versnel, H., Prijs, V. F., & Schoonhoven, R. (1992). Round-window recorded potential of single-fibre discharge (unit response) in normal and noise-damaged cochleas. *Hearing Research*, *59*(2), 157–170.